

Densification and Shape Distortion of the Al-Cu-Mg Pre-Alloyed Powder Compact in Supersolidus Liquid Phase Sintering Process

H. Momeni, S. G. Shabestari* and S. H. Razavi

* shabestari@iust.ac.ir

Received: June 2020

Revised: August 2020

Accepted: September 2020

* School of Metallurgy and Materials Engineering, Iran University of Science and Technology (IUST), Narmak, Tehran, Iran

DOI: 10.22068/ijmse.17.4.87

Abstract: In this research, densification and shape distortion of the Al-Cu-Mg (Al2024) pre-alloyed powder compact in the supersolidus liquid phase sintering (SLPS) process were investigated. The effect of Sn on the sintering process was also studied. The powders were compacted at pressures ranging from 100 to 500 MPa in a cylindrical die. The sintering process was performed in a dry N₂ atmosphere at various temperatures (580-620 °C) for 30 min at a heating rate of 10 °C min⁻¹. Results showed that the onset of the densification process was observed at 600 °C and the onset of distortion occurred at 610 °C. Addition of 0.1 wt. % Sn to the alloy has increased the distortion of the samples produced from Al-Cu-Mg pre-alloyed powder, but their densification has been improved. The compact pressure of 200 MPa caused the complete densification at the optimum sintering temperature and the compact pressures greater than 200 MPa; the sintered density was independent of green density.

Keywords: Al-Cu-Mg, SLPS, distortion, densification.

1. INTRODUCTION

Complex aluminum alloy components fabricated by powder metallurgy (P/M) offer the promise of a low cost and high strength-to-weight ratio, which meets the demands of the automotive sector [1]. During the last decade, interest in sintered aluminum-based structural parts for industrial applications has been increased [2, 3]. Successful sintering of aluminum alloys can only be achieved through the formation of a liquid phase [2]. Supersolidus liquid phase sintering (SLPS) is an impressive process to produce sintered aluminum-based parts.

Distortion severely limits the use of powder compaction following the SLPS process as a net shaping process. Therefore, understanding the distortion of the parts is important for producing high-quality parts. Studies on SLPS systems showed the sintering window concept which helps us to determine the temperature beyond which distortion occurs [4]. German [4] has reported that a critical range for fractional grain boundary coverage by liquid ($0.89 < F_C < F_{dist}$) exists in which densification occurs without the concomitant distortion due to creep mechanisms. Liu et al. [5] proposed a microstructural softening parameter ζ , which combines the effects of grain size, liquid volume fraction, and contiguity to

separate densification and distortion. ζ is given by:

$$\zeta = \frac{G^{\frac{1}{3}} V_L}{3 V_S} \quad (1)$$

Where G is the grain size, V_L is the liquid volume fraction and V_S is the solid volume fraction. The ideal sintering condition occurs for:

$$\zeta_{densif} \leq \zeta \leq \zeta_{distort} \quad (2)$$

Schaffer and Huo found that differential shrinkage during sintering and cooling rate from sintering temperature are two predominant causes to distort Al-Zn-Mg-Pb alloys [6].

It is widely known that the addition of traces of some elements can enhance the wettability of the liquid phase which is the main condition for a successful liquid phase sintering [7, 8]. Most studies of the sintering characteristics of aluminum alloy focus on the liquid phase sintering of aluminum alloy blended powder [8-10]. Compaction pressure, sintering temperature, and sintering atmosphere are key parameters to produce high-quality parts via the press-sinter route. Heard et al. determined that the optimum compaction pressure was 600 MPa for Alumix-231 (Al- 2.5%Cu- 0.5%Mg- 14%Si) [11]. The

best-sintered properties of aluminum-based compacts are achieved by sintering in dry nitrogen [7, 8, 12]

There is few published paper which systematically describes the effect of SLPS process and addition of trace element (Sn) on the distortion of Al-Cu-Mg aluminum alloy. In the present paper, the effect of compact pressure and sintering temperature has been investigated on the dimensional stability of the sintered parts made of Al-Cu-Mg aluminum pre-alloyed powder during SLPS with and without tin addition.

2. EXPERIMENTAL METHODS

Air atomized Al-Cu-Mg (Al2024) alloy powder with the chemical composition given in Table 1 was used. The particle size of powder used in the present study was less than 100 μm . 0.1 wt. % Sn powder having a size less than 71 μm was used as a trace addition and mixed with the pre-alloyed powders in a tubular mixer for 30 minutes. Oleic acid was used as a die wall lubricant.

Table 1. Composition of pre-alloyed 2024 aluminum alloy (wt. %).

Al	Cu	Mg	Si	Fe	Mn
Balance	3.95	1.23	0.45	0.27	0.36

Melting characteristics were determined using a differential thermal analysis (DTA). Dilatometry was carried out on the cylindrical samples having a 4 mm diameter and 10 mm length with a green density of 2.35 g cm^{-3} . The powders were compacted at pressures ranging from 100 to 500 MPa in a cylindrical die having an internal diameter of 12 mm for other studies. The green density was determined from weight and dimensional measurements with the accuracy of ± 0.001 g and ± 0.001 mm, respectively. Samples were preheated for 20 min at 300 $^{\circ}\text{C}$. The sintering process was performed in a dry N_2 atmosphere at various temperatures ranging from the solidus to liquidus temperatures for 30 min at a heating rate of 10 $^{\circ}\text{C min}^{-1}$. The sintered density was measured using the Archimedes method (ASTM B328). The distortion is defined as the ratio of the maximum diameter (D_{max}) to the minimum diameter (D_{min}) of a cylindrical compacted specimen.

Contiguity (C_{SS}) is defined as the fraction of the internal surface area of a phase shared with grains of the same phase in a dual-phase microstructure. The fractional grain boundary coverage (FC) by the liquid is defined as: $\text{FC} = 1 - C_{\text{SS}}$ [13]. Contiguity was calculated by counting the number of solid-solid (N_{SS}) and solid-liquid (N_{SL}) interfaces intersected by random lines superimposed on the microstructure using the following formula:

$$C_{\text{SS}} = \frac{2N_{\text{SS}}}{N_{\text{SL}} + 2N_{\text{SS}}} \quad (3)$$

3. RESULTS AND DISCUSSION

The DTA plots obtained for air atomized Al-Cu-Mg (Al2024) alloy powder are shown in Fig. 1. The solidus and liquidus temperatures were determined to be 560 and 640 $^{\circ}\text{C}$, respectively. The liquid volume fraction at a particular temperature above the solidus can be estimated by the ratio of the partial peak area to the total peak area of the DTA curve [14].

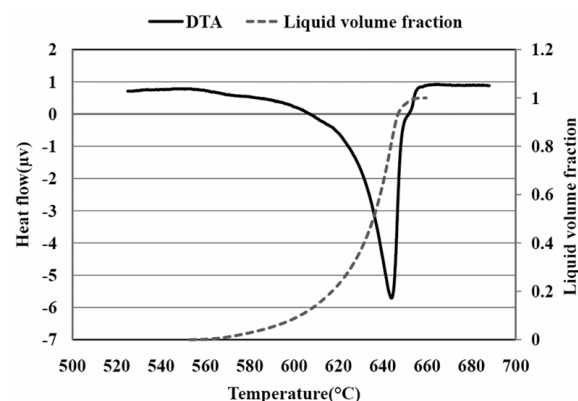


Fig. 1. DTA plot and liquid volume fraction showing melting behavior of air atomized Al-Cu-Mg (Al2024) alloy powder.

In Fig. 1 the amount of liquid was increased with the temperature above the solidus temperatures. At temperatures ranging from 580 to 620 $^{\circ}\text{C}$, the rate of liquid volume fraction that increases with temperature ($dV_L/dT = 0.6 \text{ \%}/^{\circ}\text{C}$) is desirable for better control of densification and dimensional precision during sintering. Because a higher rate could lead to a large amount of liquid in a narrow temperature range, leading to microstructural coarsening, and poor dimensional control. Dilatometry tests were performed on the compacted specimens having 0.1 wt.% Sn by

heating them to 610 °C at the heating rate of 10 °C/min. The results are shown in Fig. 2. The samples made of air atomized Al-Cu-Mg with 0.1 wt. % Sn show rapid densification starting at 560 °C and full densification is obtained at 610 °C. These results are consistent with the findings of Cook et al. [3], who improved the densification of the 2618 aluminum alloy by adding tin to the sintering process.

A peak in the shrinkage rate curve indicates the temperature (610 °C) at which the most intensive sintering condition occurs. It is worth mentioning that although fully dense samples are achieved; also they are distorted.

This is due to several factors, such as increasing liquid content with temperature, grain growth, and decreasing viscosity.



Fig. 2. Dilatometric plot of the shrinkage and shrinkage rate of the samples made of air atomized Al-Cu-Mg alloy powder having 0.1wt. %Sn heated at 10°C/min.

Fig. 3 shows the changes in the relative density and distortion of the parts which were compacted at a pressure of 300 MPa and sintered at temperatures ranging from 580 to 620 °C.

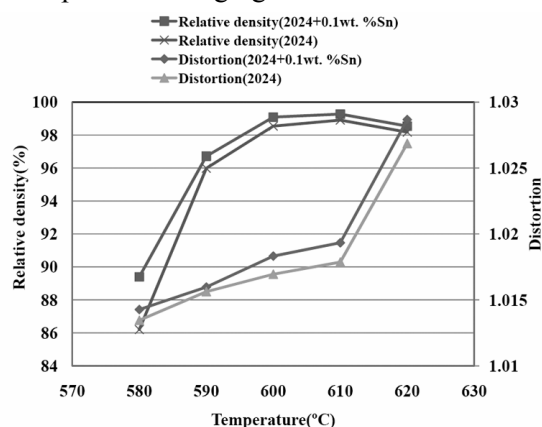


Fig. 3. Relative density and distortion versus sintering temperature of the parts produced from air atomized Al-Cu-Mg (Al2024) alloy powder with and without Sn.

The density of the sintered samples increases rapidly due to particle rearrangement and bulk shrinkage that was progressed by the supersolidus liquid phase which formed at 610 °C. The high sintered density with minimum distortion is obtained at 600 °C. On the other hand, there is a rapid increase in distortion at temperatures above 610 °C. Thus, there is a sintering temperature window where precise high-density compacts are obtained.

Distortion occurs after full densification. After densification, the compacted samples consist of solid grains with the liquid film along the grain boundaries. The evolution of the microstructure of the specimens during sintering is shown in Fig. 4. The liquid eutectic phases are presented along the grain boundaries. With increasing sintering temperature, this liquid phase spreads along the grains and causes distortion when the liquid covers the majority of the grain boundaries. Once the pores are filled, the capillary force approaches zero; while the gravitational force exceeds the in situ compact strength and therefore results in distortion [15]. Grain growth is a dominant aspect of microstructural evolution that occurs with the liquid formation and spreading during SLPS.

Fig.5 shows the effect of sintering temperature on the grain size of the samples. The grain size has been increased by sintering temperature. According to Fig.4, grain coarsening, pore coalescence, and therefore, reduction in relative density occurs with increasing the temperature to greater than 610 °C (Fig. 3).

The fractional grain boundary coverage by liquid was increased with the addition of 0.1 wt. % Sn (Fig. 6). It is not expected that 0.1 wt. % Sn increases the liquid volume fraction noticeably. Tin has a higher vacancy binding energy and a higher diffusivity in Al than Cu does [16]. The liquid persists for longer times, improving the fractional grain boundary coverage and results in improved densification; but distortion and grain size are increased.

From Fig. 3 and Fig. 6, it can be concluded that distortion occurs at temperatures that fractional grain boundary coverage is greater than 0.90. This result is in good agreement with the German model [4]. The onset of densification was observed at 600 °C and the onset of distortion was 610 °C. Microstructural softening parameter ζ has been calculated using equation (1) as:

$$\zeta_{\text{densif}} = 0.09 \mu\text{m}^{(1/3)}$$

$$\zeta_{\text{dist}} = 0.17 \mu\text{m}^{(1/3)}$$

Thus, densification with minimum distortion occurs for:

$$0.09 \leq \zeta \leq 0.17$$

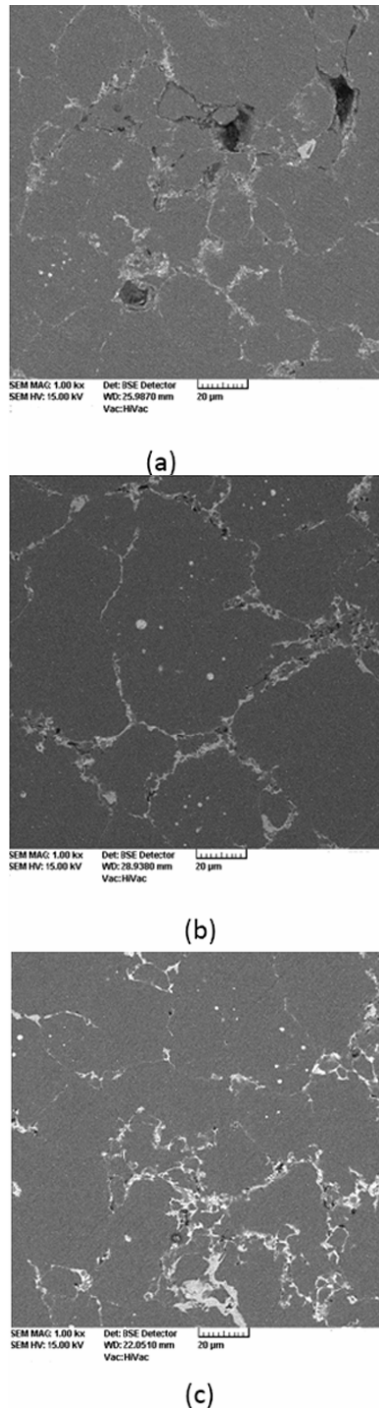


Fig. 4. BSE images of the specimens made of Al-Cu-Mg aluminum alloy powder having 0.1 wt. % Sn sintered at various temperatures and water quenched. a) 580 °C, b) 610 °C, c) 620 °C

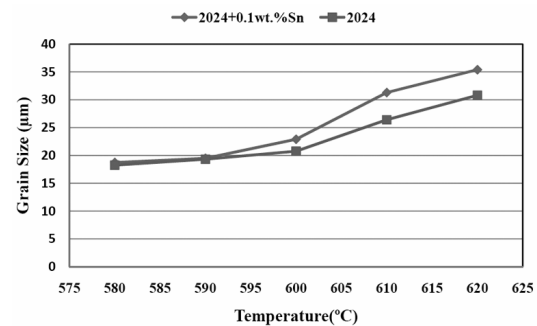


Fig. 5. Grain size as a function of sinter temperature for the samples made of air atomized Al-Cu-Mg aluminum alloy powder with and without Sn.

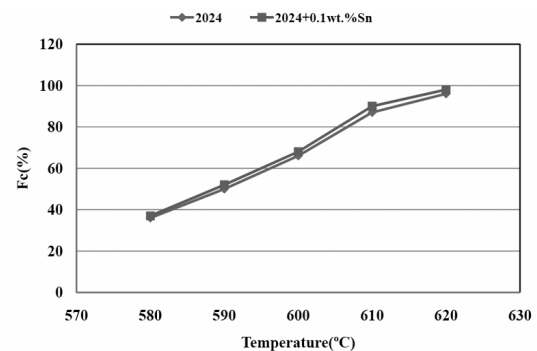


Fig. 6. Fractional grain boundary coverage by liquid as a function of sinter temperature for the samples made of air atomized Al-Cu-Mg aluminum alloy powder with and without Sn.

Fig. 7 shows the influence of compaction pressure on the green density, sintered density, and distortion. When the samples sintered at the optimum sintering temperature of 610 °C, the samples compacted at lower pressure shrink more than those compacted at higher pressures. Therefore, the rate of densification was increased in the lower pressure compacted samples. The green density increases with compaction pressure while, at compaction pressures greater than 200 MPa, the sintered density is independent of green density.

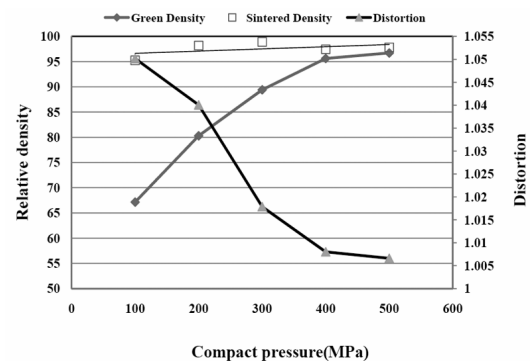


Fig. 7. Green and sintered density (sintered at 610 °C) and distortion as a function of compaction pressure for the samples made of air atomized Al-Cu-Mg aluminum alloy powder.

It seems that at compaction pressures 200 MPa breaking down of most oxide layers has occurred and this phenomenon causes full densification at optimum sintering temperature. At higher pressures, the green density increases but the density of the sintered samples does not change significantly.

To achieve a full density in the sintered parts, more dimensional change occurs when the compaction pressure is low. It is because at higher compaction pressure, the samples have less free volume for the new liquid to fill, and consequently the contiguity increases while the distortion decreases.

Green density gradient is greater at low compaction pressures. These green density differences cause non-uniform dimensional changes to occur. This distortion can be minimized by high compaction pressures.

4. CONCLUSION

Based on the results obtained in this research, conclusions are as follows:

1. The onset of densification was observed at 600 °C and the onset of distortion was 610 °C
2. The rate of densification was increased in the lower pressure compacted samples.
3. The optimum sintering condition for the control of dimensional stability and achieving a full density in the sintered parts occurs where the microstructural softening parameter, ζ is in the range of:
$$0.09 \leq \zeta \leq 0.17$$
4. Distortion of samples produced from Al-Cu-Mg pre-alloyed powder was increased with the addition of 0.1 wt. % Sn, however, their densification was improved.
5. The compaction pressure of 200 MPa, causes complete densification at the optimum sintering temperature and compaction pressures greater than 200 MPa and the sintered density is independent of green density.
6. By applying the optimum condition, fully dense sintered parts can be produced by Al-Cu-Mg (Al2024) pre-alloyed powder compact.

REFERENCES

1. Arockiasamy, A., German, R.M., Wang, P., Horstemeyer, M.F., Morgan, W. and Park, S. J., "Sintering behaviour of Al-6061 powder produced by rapid solidification process", Powder Metall., 2011, 54 (3), 354-359.
2. Tingting, Q., Mao, w., Zhiyuan, D., Xuanhui, Q., "Microstructure evolution and densification behaviour of powder metallurgy Al-Cu-Mg-Si alloy", Powder Metallurgy, 2020, 63(1), 54-63.
3. Cooke, R. W., Hexemer, R. L., Donaldson, I. W., Bishop, D.P., "Press-and-sinter processing of a PM counterpart to wrought aluminum 2618", J. mater . process.tech, 2016,230, 72-79.
4. German, R. M., "Supersolidus Liquid-Phase Sintering of Pre-Alloyed Powders, Metall. Mater.Trans". A, 1997, 28A, 1553-1567.
5. Liu, J., Lal, A. and German, R.M., "Densification and Shape Retention in Supersolidus Liquid Phase Sintering", Acta Metall., 1999, 47(18), 4615-4626.
6. Schaffer, G. B. and Huo, S. H., "Distortion In A Sintered 7000 Series Aluminum Alloy", Powder Metall., 2000, 43(2), 163-167.
7. Schaffer, G. B., Yao, J. -Y., Bonner, S. J., Crossin, A. E., Pas, S. J. and Hill, A. J., "The effect of tin and nitrogen on liquid phase sintering of Al-Cu-Mg-Si alloys", Acta Mater., 2008, 56,2615-2624.
8. MacAskill, I. A., Hexemer, R. L., Donaldson, I. W., and Bishop, D. P., "Effects Of Magnesium, Tin And Nitrogen On The Sintering Response Of Aluminum Powder", J.Mater. Process.Tech., 2010, 210, 2252–2260.
9. Dunnetta, K.S., Muellera, R.M. and Bishopb, D.P., "Development of Al-Ni-Mg-(Cu) Aluminum P/M Alloys", J.Mater. Process.Tech., 2008, 198, 31–40.
10. Showaiter, N. and Youseffi, M., "Sintering and Mechanical Properties of Elemental 6061 Al Powder With And Without Sintering Aids", Materials and Design., 2008, 29, 752-762.
11. Heard, D. W., Donaldson, I. W. and Bishop, D. P., "Metallurgical Assessment Of A Hypereutectic Aluminum-Silicon P/M Alloy", J. Mater. Process. Tech., 2009, 209, 5902–5911.

12. Pieczonka, T., Schubert, Th., Baunack, S. and Kieback, B., "Dimensional Behaviour Of Aluminum Sintered In Different Atmospheres", *Mater. Sci. Eng. A.*, 2008, 478, 251-256.
13. German, R. M., "Sintering Theory And Practice", New York, Wiley, 1996, 230-236.
14. Lal, A., Iacocca, R. G. and German, R. M., "Densification During The Supersolidus Liquid Phase Sintering Of Nickel-Based Pre-Alloyed Powder Mixtures", *Metall. Mater.trans. A*, 1999, 30A, 2201-2207.
15. Liu, Y., Tandon, R. and German, R. M., "Modeling Supersolidus Liquid Phase Sintering: Densification", *Metall. Mate. Trans. A*, 1995, 26A, 2423-2430.
16. Sercombe, T. B. and Schaffer, G. B., "The Effect of Trace Elements On The Sintering Of Al-Cu Alloys", *Acta Mater*, 1999, 47, 689-697.

